DUCTILE SEISMIC RETROFIT OF STEEL DECK-TRUSS BRIDGES. I: STRATEGY AND MODELING

By Majid Sarraf[1] and Michel Bruneau,[2] Members, ASCE

ABSTRACT: Most deck-truss bridges have been designed and constructed without seismic resistance considerations; as a result, their members, connections, and frequently their substructure are not sized and detailed to provide the ductile response needed during major earthquakes. A ductile seismic retrofit solution proposed here consists of converting the deck slab into a composite slab and replacing the end cross-frames and the lower lateral braced panels adjacent to the supports by special ductile diaphragms, thus creating ductile fuses to protect the remaining superstructure and substructure. This paper illustrates the typical seismic vulnerability of such bridges, presents a model governing transverse seismic response of retrofitted deck-trusses, and a methodology to determine overall stiffness and strength of such ductile panels based on developed seismic performance goals. The results of computer simulations for a retrofitted deck-truss subjected to severe ground excitation validates the proposed methodology and the global modeling. It is concluded that the proposed ductile retrofit solution can significantly enhance seismic performance of deck-trusses.

INTRODUCTION

A large number of steel bridges have been designed and constructed at a time when bridge codes had no seismic design provisions, or when these provisions were inadequate by today's standards. Many of these bridges will suffer severe damage when struck by earthquakes, as evidenced by some recent moderate earthquakes (Astaneh-Asl et al. 1994; Housner and Thiel 1995; Bruneau et al. 1996).

Among all types of steel bridges, deck-truss bridges are particularly vulnerable. Typically, in these structures constructed for many decades throughout North America, the deck is seated on the truss structure, which is supported on abutments or piers. Hence, seismically induced inertia forces in the transverse direction at deck level act with a sizable eccentricity with respect to the truss reaction supports, and the entire superstructure is mobilized to transfer these forces from deck to supports. The top and lower lateral bracings, end and interior cross-frame bracings, and other lateral-load resisting components in these older bridges, designed only to resist wind forces, would be unable to withstand the severe cyclic inelastic behavior expected to develop during large earthquakes. Moreover, these spans are often supported on nonductile substructures.

Recent seismic evaluations of deck-truss bridges have typically revealed the need to replace and/or reinforce many of the superstructure members and substructure components (Table 1). This can be expensive, particularly when work is required in difficultly accessible parts of the bridge; strengthening approaches also require conservative scenarios of future earthquake occurrence, because they cannot guarantee adequate seismic performance beyond the threshold of damage. In most cases, base isolation has been recommended for deck-truss bridges (Table 2). However, while effective, this retrofit strategy can also be costly as it sometimes requires extensive abutment modifications and superstructure changes; in some projects, base isolation proved to be more expensive than conventional strengthening [e.g., Capron (1995) and Matson (1995)].

To provide for an alternative and potentially more economical solution, a capacity-based seismic retrofit procedure is proposed here to protect both the superstructure and substructure, by introducing ductile steel energy-dissipating elements at judiciously selected locations into the superstructure. These special ductile elements, detailed to reliably dissipate seismic energy through the development of stable hysteretic behavior, are used as a mechanism to prevent yielding in other parts of the structure, thereby acting as structural fuses. To achieve this capacity protection in steel deck-truss bridges, the retrofit scheme proposed here requires conversion of the deck slab into a composite slab (as recently done to some bridges in Canada), replacement of the end cross-frames by special ductile panels, and replacement of the last lower lateral braced panels near the piers by similarly conceived ductile panels. These specially designed ductile diaphragms and panels are calibrated to yield before the strength of the substructure is reached and prior to the development of any undesirable failure modes in the superstructure. Contrary to some of the existing alternatives, retrofit work is only required at easily accessible superstructure locations.

In this paper, following identification of the multiple load paths contributing to seismic resistance in deck-truss bridges, and formulation of a simplified model of that behavior, a design procedure for the proposed seismic retrofit solution is presented. This procedure accounts for all strength and stiffness constraints on the retrofit solution. Finally, to illustrate the effectiveness of the proposed retrofit strategy, nonlinear analysis is conducted for a generic deck-truss bridge retrofitted using idealized ductile panels. The design of actual passive energy dissipation systems for these ductile panels is the subject of a subsequent paper (Sarraf and Bruneau 1998) because it requires consideration of a number of additional design constraints tied to the type of ductile device chosen.

Note that the proposed retrofit strategy only provides enhanced seismic resistance and substructure protection for the component of seismic excitation transverse to the bridge, and it must be coupled with other devices that constrain longitudinal seismic displacements, such as simple bearings strengthening (Mander et al. 1996), rubber bumpers, etc. Transportation agencies experienced in seismic bridge retrofit have indicated that deficiencies in the longitudinal direction are typically much easier to address than those in the lateral direction (Radloff, Seismic Rehabilitation Engineer, Ministry of Transportation of British Columbia, 1996, private communication). Also, note that, in this study, the truss superstructure is taken as seated on nonductile but stiff abutments or piers, whose

[1]PhD Candidate/Lecturer, Ottawa-Carleton Earthquake Engrg. Res. Ctr., Dept. of Civ. Engrg., Univ. of Ottawa, Ottawa, Ontario, Canada K1N 6N5. E-mail: msarraf@uottawa.ca

[2]Prof., Ottawa-Carleton Earthquake Engrg. Res. Ctr., Dept. of Civ. Engrg., Univ. of Ottawa, Ottawa, Ontario, Canada K1N 6N5.

Note. Associate Editor: Sashi K. Kunnath. Discussion open until April 1, 1999. Separate discussions should be submitted for the individual papers in this symposium. To extend the closing date one month, a written request must be filed with the ASCE Manager of Journals. The manuscript for this paper was submitted for review and possible publication on February 18, 1998. This paper is part of the *Journal of Structural Engineering*, Vol. 124, No. 11, November, 1998. ©ASCE, ISSN 0733-9445/98/0011-1253–1262/$8.00 + $.50 per page. Paper No. 17812.

TABLE 1. Seismic Evaluation of Deficiencies in Deck-Truss Bridges

Deficiencies (1)	Bridge (Span Location)				
	Bencia-Martinez[a] (main) (2)	Burrard[b] (main and approach) (3)	Granville[b] (main and approach) (4)	Second Narrows[b] (approach and main) (5)	Golden Gate[c] (North approach) (6)
Bearings	x	x	x	x	x
Piers or bents	x	x	x	x	x
Top and bottom lateral bracings	x	x	x	x	x
Interior cross-frames	x			x	x
End cross-frames	x				x

[a]From Imbsen and Liu (1993) and Liu et al. (1997).
[b]From Matson and Buckland (1995).
[c]From Imbsen (1995).

TABLE 2. Retrofit Strategies for Deck-Truss Bridges

Retrofit strategies (1)	BRIDGE (SPAN LOCATION)						
	Bencia-Martinez[a] (Main)		Burrard[b] (Main and Approach)	Granville[b] (Main and Approach)	Second Narrows[b] (Approach)	Second Narrows[b] (Main)	Golden Gate[c] (North Approach)
	Option 1 (2)	Option 2 (3)	Option 1 (4)	Option 1 (5)	Option 1 (6)	Option 2 (7)	Option 1 (8)
Isolation bearings (rubber/yielding devices)		x	x		x		x
Sliding/frictional bearings	x			x			
Strengthening piers	x	x	x	x	x	x	x
Strengthening bearings	x					x	
Strengthening top/bottom laterals	x		x	x		x	x
Strengthening interior cross-frames	x	x				x	x
Strengthening end cross-frames						x	x

[a]From Imbsen and Liu (1993) and Liu et al. (1997).
[b]From Matson and Buckland (1995).
[c]From Imbsen (1995).

flexibility has a negligible effect on global dynamic response. Therefore, substructure stiffness is not included in the model. Nonetheless, the retrofit strategy proposed here accounts for the limited substructure strength available and the need to prevent structural damage there.

SEISMIC BEHAVIOR OF EXISTING DECK-TRUSS BRIDGES

Inelastic analyses of a representative deck-truss bridge were conducted using the program DRAIN-3DX (Prakash et al. 1994) to illustrate typical nonlinear behavior, to show the location and magnitude of structural deficiencies, and to allow full appreciation of how effectively the proposed retrofit strategy can enhance seismic resistance. The generic deck-truss bridge considered, constructed using information taken from structural drawings supplied by practicing engineers under confidentiality agreements, has an 80 m span and is 10 m tall and 10 m wide. The truss panels on all sides are 10 m × 10 m in size. The 225-mm-thick concrete deck is discontinuous due to the presence of expansion joints at each panel joint (10 m). This deck-truss is supported on two bearings on abutments at each of its end. At these supports, vertical and transverse displacement of the joints are restrained, and horizontal displacements along the longitudinal axis of the truss are allowed at one end. The truss members are modeled by elements exhibiting elastic buckling in compression and elasto-perfectly-plastic behavior with 3% strain hardening in tension.

The nonlinear inelastic analysis of this deck-truss bridge subjected to the El Centro 1940 N-S excitations scaled to a peak ground acceleration of 0.5*g* revealed that many end cross-frame braces, verticals, top laterals, interior cross-frame braces, and lower laterals, buckled and yielded, with member ductility demands sometimes in excess of 8. The locations of damage throughout the bridge are identified in the exploded

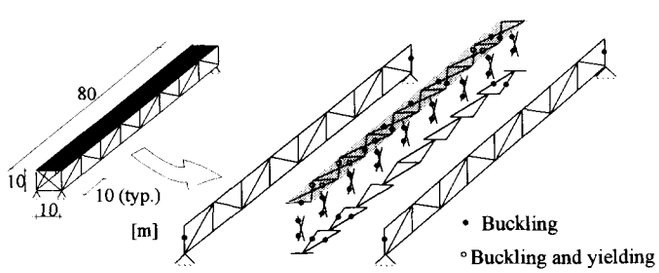

FIG. 1. Damaged Members in Deck-Truss Bridge Subjected to 0.5*g* El Centro Earthquake

view of the deck-truss shown in Fig. 1. Maximum values of ductility demand for top lateral braces is 3.5, for yielding in tension, and 8.2, 3.4, 3.3, 3.3, and 7.5, respectively, for buckling of the top lateral braces, end cross-frame verticals, end cross-frame braces, interior cross-frame braces, and lower lateral braces. Results also showed a significant midspan displacement relative to the ends as a consequence of the large flexibility of the top lateral resisting system. This translates into a greater share of the seismically induced inertia force flowing into the lower laterals through the interior cross-frames (i.e., sway-frames). Note that this simple analysis neglects many other deficiencies commonly encountered in deck-truss bridges (e.g., connections unable to develop member strengths) that would require consideration by the engineer in assessing the seismic retrofit needs.

SEISMIC LOAD PATHS IN DECK-TRUSS BRIDGES AND CONCEPTUAL TWO-DIMENSIONAL (2D) MODEL

A series of preliminary elastic analyses conducted using the general purpose structural analysis program SAP90 (Wilson and Habibullah 1990) revealed the existence of two dominant load paths contributing to the seismic resistance of deck-truss

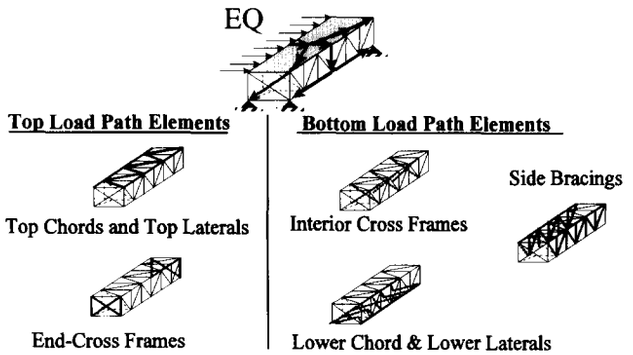

FIG. 2. Seismic Load Paths in Deck-Truss Bridges

bridges. As illustrated in Fig. 2, structural elements along the first path, referred to hereafter as the top load path, consist of top laterals and end cross-frames. The second path of seismic resistance, defined as the bottom load path, is provided by the combined action of the interior cross-frames with the exception of the last braced bay, and the lower laterals. As described in more detail in a later section, the seismic resistance of deck-truss bridges also engages to some extent the torsional resistance provided by the trussed box action of the structural system. This torsional resistance was found to depend on the vertical side bracings of the truss; these are considered part of the lower load path since the top load path behavior was found to be insensitive to variations in stiffness of the side bracings.

The lateral loads resisted by the individual load paths were found to depend in a complex manner on the stiffness of the different structural components along each path, according to an overall system behavior that can be conceptually expressed by the 2D model shown in Fig. 3. In this model:

- The top beam simulates the flexural behavior of the top lateral horizontal truss system (top truss), consisting of top chords and top laterals, directly subjected to the lateral inertia forces of the deck.
- The lower beam simulates the flexural behavior of the lower chords and lower lateral horizontal truss system (lower truss) subjected to the horizontal component of the seismic forces transferred by the interior cross-frames.
- Each spring connecting the top and bottom beam represents the transverse stiffness of an interior cross-frame.
- The end springs model the end cross-frames, usually stiffer than the interior cross-frames, transferring the loads directly to the bridge supports.

This 2D model is not used for the nonlinear analyses reported in this paper but is useful to qualitatively illustrate the impact of various structural changes on structural behavior.

Analyses were conducted to investigate whether stiffening and strengthening of a single load path, to attract and resist most of the seismic loads, could lead to a reduced demand and eliminate the need for retrofit along the other load path. This is not the case, and the conceptual 2D model can be used to explain the problems associated with this approach.

Consider strengthening of the top load path. As shown in bold in Fig. 4(a), this corresponds to strengthening of the top beam (i.e., top lateral truss) and its spring supports (i.e., end cross-frames) on the 2D model. Although some stiffening nat-

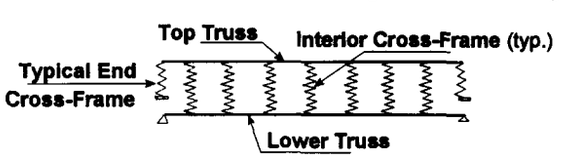

FIG. 3. 2D Model of Deck-Truss Bridge

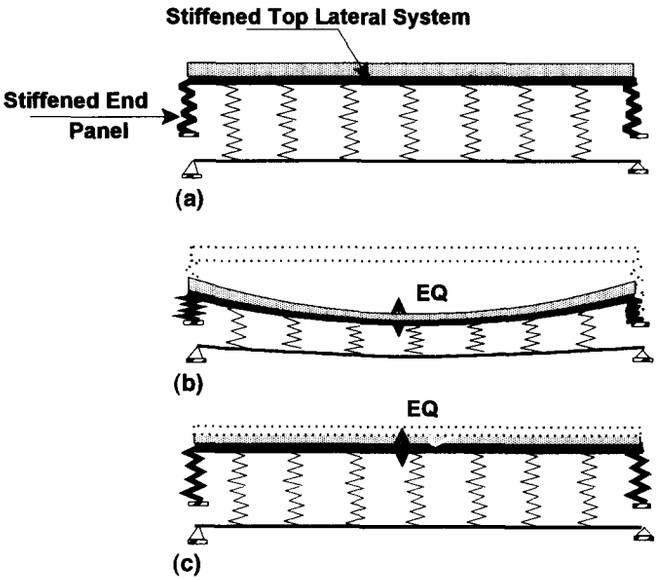

FIG. 4. Strengthening of Top Load Path Alone: (a) Strengthened Elements in Bold (End Springs and Top Beam); (b) Large Deformations in Interface Springs and Top Beam; (c) Considerable Stiffening of Top Beam and End Springs

urally results from the strengthening of these elements, the flexural deformation of the top beam remains sufficiently large to impose large deformations (and subsequently excessive forces and damage) in the interface springs between the top and lower beams [Fig. 4(b)]. Thus, further strengthening of the top beam and end springs is required for the sake of increasing stiffness to reduce the magnitude of the deformations imposed on the lower system. This, in turn, also changes the overall stiffness of the structure, reduces its period of vibration, and may increase the overall inertia forces, resulting in an increased force demand in the top beam and end springs, which then again require further strengthening. Parametric studies showed that a prohibitive stiffening is required to achieve the ideal situation shown in Fig. 4(c) in which no damage develops in the lower load path.

Strengthening the lower load path system alone is even a poorer choice. Fig. 5(a) shows, in bold, the corresponding strengthened elements in the 2D model. Note that many of the structural members in the lower load path (e.g., interior cross-frames and lower laterals) are often small and very slender sections originally designed only to resist wind loads, and excessive strengthening is required to make that load path dominant. Parametric studies indicate that even with a significant increase in the stiffness and strength of these elements, there is still a large force transferred to the top load path [Fig. 5(b) schematically illustrates this behavior]. Interestingly, even with a lower lateral truss and interior cross-frames of infinite rigidity in the horizontal plane, the desired behavior is not attained. This is due to the torsional behavior of the entire deck-truss, which also depends on the in-plane stiffness of the side trusses [Fig. 5(c)]. Therefore, stiffening the side trusses in addition to strengthening of the lower truss and interior cross-frames would be required to achieve the desired performance [Fig. 5(d)].

Finally, as mentioned earlier, strengthening alone using any approach, without consideration of ductile behavior, cannot ensure satisfactory seismic performance of deck-trusses during earthquakes more severe than considered as the basis for retrofit.

RETROFIT USING CAPACITY DESIGN CONCEPT

A ductile retrofit scheme based on a capacity design concept is an attractive solution to minimize the extent of retrofit ac-

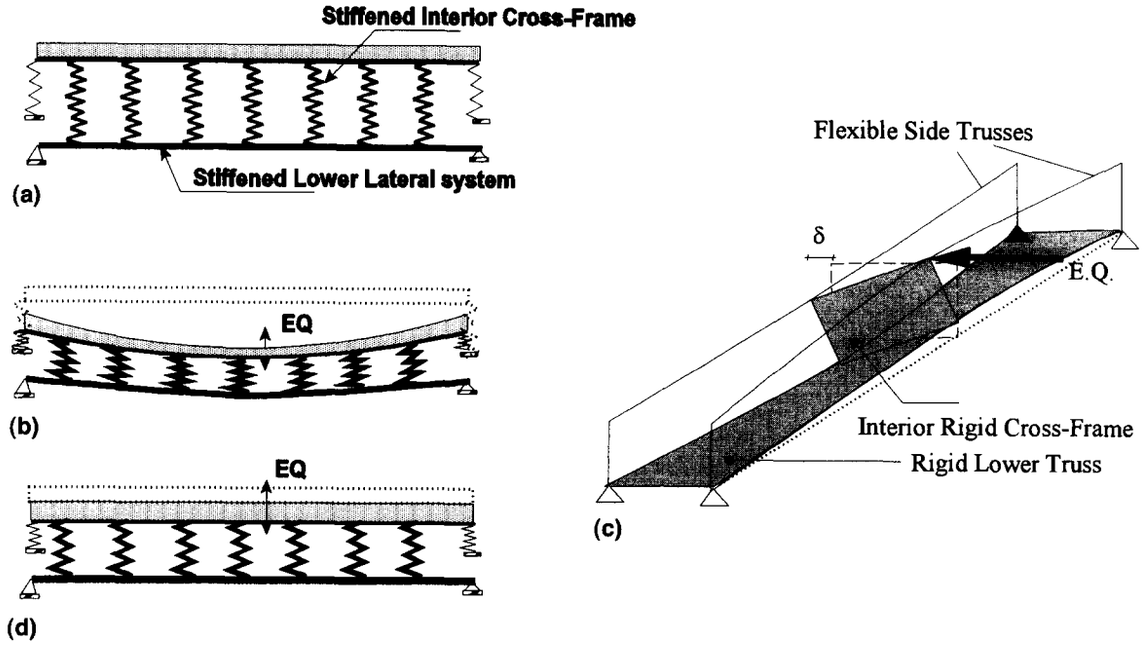

FIG. 5. Strengthening Lower Path Alone: (a) Strengthened Elements in Bold (Interface Springs and Lower Beam); (b) Large Deformation and Potential Damage of Top Beam and End Springs due to Insufficient Strengthening; (c) 3D Deformations in Spite of Infinite In-Plane Rigidity of Lower Truss and Cross-Frame, due to Torsional Flexibility of Entire Truss; (d) Side Trusses (Not Shown) Are Stiffened, in Addition to Interior Cross-Frames and Lower Lateral Truss

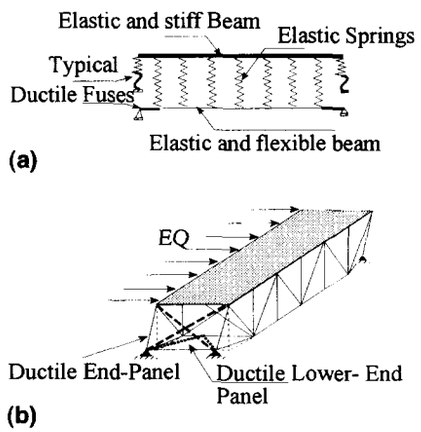

FIG. 6. Ductile Retrofit Concept: (a) in 2D Model; (b) Implementation in Actual Deck-Truss Bridge

tivities, and the benefits of this approach have been described in the Introduction section. Various schemes were considered, and analyses revealed that the best strategy was to locate yielding devices in the end-cross frames and in the lower end panels. Fig. 6(a) shows the 2D model of this concept, with ductile fuses shown in bold. Introducing two ductile yielding devices acting as fuses at each end of the two beams can limit the magnitude of forces transferred to the lower beam and the interface springs, the top beam, and end support reactions.

The implementation of this concept is shown in Fig. 6(b). It requires conversion of each end cross-frame into a ductile panel having a specially detailed yielding device (i.e, a structural fuse) and conversion of the last lower end panel near each support into a similar ductile panel. It also requires stiffening of the top truss system, which can be achieved by connecting the existing individual concrete deck panels to create a continuous deck. This stiffening has two benefits. First, for a given deck lateral displacement at the supports, it reduces midspan sway, resulting in lower forces in the interior cross-frames. Second, it increases the share of the total lateral load transferred by the top load path. Interestingly, once the deck is made continuous and well tied to the truss, the in-plane flexural stiffness of the top truss becomes sufficiently large to be modeled as a rigid beam in the 2D model. This greatly simplifies the derivation of expressions for the generalized stiffness and fundamental period of the retrofitted structure.

DESIGN CONSTRAINTS FOR SELECTION OF RETROFIT SYSTEM

Seismic performance of the retrofitted superstructure varies as a function of the values of stiffness and strength of the ductile end and lower panels. Thus, these values must be carefully determined by the engineer. Any type of ductile energy dissipation system could be implemented in the end panels and lower end panels of the deck-truss, as long as its stiffness and strength characteristics satisfy the following requirements.

Strength Requirements

In a capacity design perspective the strength requirements are as follows:

- Strength of the retrofitted lower end panels must be chosen to limit the force demand in the interior cross-frames and lower truss and ensure that these remain elastic, for any seismic excitation.
- Strength of the retrofitted end cross-frames must be chosen to ensure that the horizontal transverse force transferred to these panels does not produce buckling of the end verticals, nor exceed the resistance of the tie-down devices.
- Sum of the strengths of both ductile panels at one end of the span must not exceed the horizontal force that triggers failure of any substructure element, such as bearings and piers, and must be greater that the strength needed to resist wind loads.

Stiffness Requirements

Some restrictions on stiffness are necessary to prevent excessive ductility demands in the retrofitted panels and exces-

sive drift and deformations in other parts of the superstructure. The engineer must identify the displacement constraints appropriate to specific bridges; these will vary depending on the detailing conditions germane to the particular bridge under consideration. Generally, among those limits of important consequences, the maximum permissible lateral displacement of the deck must not exceed the values at which

- P-Δ effect causes instability of the end verticals during sway of the end panel [Fig. 7(a)] or damage to the connections of the end verticals [Fig. 7(b)].
- Unacceptable deformations start to develop in members or connections of the deck-truss, such as inelastic distortion of gusset plates [Fig. 7(c)], premature bolt or rivet failures, or damage to structural members [Fig. 7(d)].
- Maximum code drift limits given in the highway bridge codes, if any, are reached (optional).
- The energy dissipating devices used in the ductile panels reach their maximum deformation without loss of strength.

The latter constraint obviously requires, for each type of energy dissipating devices considered, engineering judgment and experimental data on the device's ultimate cyclic inelastic performance, often expressed by a consensus opinion. For a given geometry, the ductility demand on the energy dissipating elements is related to the global ductility demand of the retrofitted deck-truss. Therefore, global stiffness of the structure must be determined to keep global ductility and displacement demands within reasonable limits. Stiffness of the ductile devices have a dominant effect on the overall stiffness, and this provides the control necessary for design.

Note that the global ductility limits corresponding to the response modification factors provided in the seismic design provisions for buildings were adopted in this study. By comparing elastic design response spectra with the design requirements for eccentric braced frames resistance (i.e., a structural system considered ductile for seismic resistance), it can be shown that a ductility reduction factor R_μ of 3.75 is typically used (i.e., $3.75 = 3/8 \times R_w$, where $R_w = 10$ for eccentric braced frames according to the Uniform Building Code. In Canada, a corresponding factor of 4.0 is specified, in a limit states design perspective) even though experimental research demonstrates that more ductile performance can be safely achieved. Hence, in this study, a maximum global ductility capacity of 3.75 is used for all ductile retrofit systems.

Finally, it is recommended that the stiffness of the retrofitted panels be kept proportional to their respective capacity, as much as possible, to ensure that yielding in all ductile panels occurs nearly simultaneously. This should enhance energy dissipation capability and minimize the differences in the local ductility demands between the various yielding devices. It also helps to prevent sudden changes in the proportion of the load shared between the two load paths and to minimize possible torsion along the bridge axis resulting from the instantaneous eccentricity that can develop when the end ductile panels yield first, while the lower end ductile panels are still elastic. That particular distribution of instantaneous stiffness can cause an undesirable situation similar to that shown in Figs. 5(b and c).

Note that, in this study, no explicit limit is imposed on system stiffness other than those resulting indirectly from the aforementioned constraints.

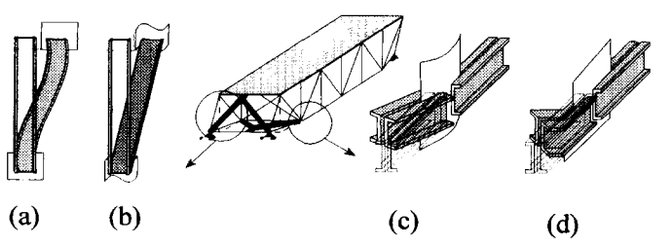

FIG. 7. Displacement Limits to Prevent: (a) Excessive Drift of End Verticals; (b) Damage of Vertical Joints due to Excessive Drift; (c) Failure of Lower Chord Joints; (d) Failure of Lower Chord Members

DESIGN PROCEDURE

A design procedure has been developed to achieve the desired performance objectives while respecting the aforementioned constraints. The basic approach is to compare equations expressing the stiffness and strength characteristics of all retrofitted panels with their respective limits and to select system properties to satisfy all of these inequalities. Closed-form solutions for the fundamental period and lateral stiffness of retrofitted deck-trusses are subsequently derived for that purpose. A graphical design approach is recommended and illustrated using Newmark-Hall design spectra.

Prediction of Lateral Period of Vibration

To calculate the fundamental period using a closed-form solution, a mathematical expression for the global lateral stiffness of the retrofitted deck-truss is necessary. Taking advantage of the relatively large rigidity of the top truss system resulting from its conversion into a continuous composite concrete deck, the dynamic behavior of the retrofitted deck-truss can be modeled as shown in Fig. 8(a). In Fig. 8, $K_{L,B}$ represents the lateral stiffness of each panel of the lower lateral system. The stiffness of each such panel is almost equal to the contribution of the braces to its stiffness. Note that brace members are often identical in all panels because, in most deck-truss bridges, their design was governed by minimum requirements. $K_{C,B}$ represents the stiffness of the cross bracing panels, also nearly equal to the contribution of the braces to the panel stiffness. Braces in those panels are also often identical in all panels, being sized to comply with minimum design requirements. In such a case, the subsystem consisting of the interior cross-frames and lower truss combined can be modeled by a series of springs. The configuration of only half of the subsystem is shown in Fig. 8(b). The equivalent stiffness for the first i springs of half of the subsystem is

$$K_i^* = \frac{K_{L,B} \cdot K_{i-1}^*}{K_{L,B} + K_{i-1}^*} + K_{C,B} \tag{1}$$

When the number of springs in that series is infinite, K_i^* is nearly equal to K_{i-1}^*, i.e., the equivalent stiffness becomes independent of the number of springs. Practically three or four lower lateral panels are sufficient to provide sufficient accuracy in this procedure. Therefore, by equating $K^* = K_{i-1}^* \simeq K_i^*$, in (1) one can obtain

$$K^* = \frac{K_{C,B} + \sqrt{K_{C,B}^2 + 4K_{C,B} \cdot K_{L,B}}}{2} \tag{2}$$

By the same logic, the global stiffness of the subsystem consisting of the interior cross-frames and the lower truss $K_{L,S}$ is

$$K_{L,S} = \frac{K^* \cdot K_{L,E}}{K^* + K_{L,E}} \tag{3}$$

where $K_{L,E}$ = stiffness of the retrofitted last lower lateral panel. Thus, from this model of behavior, the global lateral stiffness of the deck-truss in the transverse direction K_{Global} is given by

$$K_{\text{Global}} = 2(K_{E,S} + K_{L,S}) \tag{4}$$

where $K_{E,S}$ = stiffness of the retrofitted end cross-frames, taking into account the contribution to stiffness of the braces,

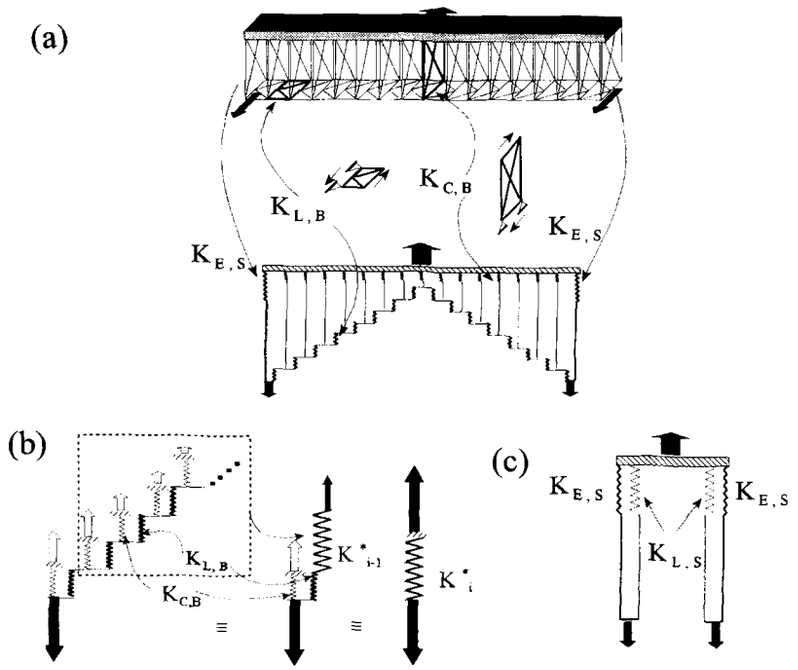

FIG. 8. Spring Models for: (a) 2D Representation of Deck Truss; (b) Interior Cross-Frame Lower Lateral Assembly; (c) Global Stiffness Model

verticals, horizontal, and ductile energy dissipation device/system, and $K_{L,S}$ is given by (3) [Fig. 8(c)].

The fundamental period for the transverse mode of vibration is then given by

$$T = 2\pi \sqrt{\frac{M}{K_{\text{Global}}}} \tag{5}$$

where M = total mass of the deck (the generalized mass in this model with rigid deck is equal to the total mass of the deck).

Note that in deck-trusses of rather long span or having relatively stiff sway bracing panels compared to the lateral flexural stiffness of the composite deck, the actual mode shape of the deck may depart more significantly from the assumed uniform transverse displacement. Also, for an end bracing panel with large height-to-width ratio, the greater eccentricity between the transversely applied inertia force and the end supports translates into a more significant twisting action and, therefore, a greater structural flexibility than captured by the simplified model that neglects this torsional stiffness. However, in both cases, the assumption of a rigid deck will lead to underestimates of the lateral period of vibration and thus higher and more conservative inertia force requirements as read from a design spectrum.

Determination of Capacity-Based Pseudoacceleration

For the reasons described earlier, the overall strength of the system, as well as that of the retrofitted panels, should be limited. To actually find these limits the following procedure is proposed:

Strength of Retrofitted End Panels

The upper limit for the transverse shear strength of each end cross-frame panel can be determined from the following:

$$V_{E,S} \leq \min\left(\frac{P_{Cr} \cdot b}{h}, \frac{T_r \cdot b}{h}\right) \tag{6}$$

where P_{cr} = critical buckling load of the end verticals including the effect of vertical gravity as well as vertical inertia force due to earthquake; T_r = tensile capacity of the tie-down device at each support; and h and b = height and width of the end cross-frame panel, respectively.

Strength of Retrofitted Lower End Panels

The maximum shear strength $V_{L,E}$ for each lower end panel is limited by the value that would trigger damage in the interior cross-frames along the lower load path (e.g., buckling of a brace in an interior cross-frame or fracture at a brace nonductile connection). Hence, to find this shear strength, the force distribution in the interior cross-frames along the span must be established. Analyses showed that this distribution is nonlinear and of a complex shape. However, an exact numerical solution to the problem is not necessary: A distribution resulting in a conservative value of $V_{L,E}$ is sufficient. Accordingly, the model used to evaluate stiffness of the lower lateral interior cross-frame subsystem (Fig. 8) is adequate if corrected as subsequently described. In that model, the shear force in the interior cross-frames reduces in magnitude, from a maximum in the first interior cross-frame panel from the support, to a minimum value in the central panel, with that minimum approaching zero as the number of panels along the span increases (practically zero for more than four panels between support and midspan). Fig 9(a) compares the actual shape of this force distribution in all interior cross-frame, with simple linear and nonlinear ones, for a given force R_1, in the first interior cross-frame from the support. Note that the ductile lower panel is designed to have strength, $V_{L,E}$, equal to $\Sigma R_i/2$. Assuming a simple linear variation of this distribution gives a maximum force in excess of the true lateral shear acting on the lower path, and R_1 would be reached prior to yielding of the ductile lower panel, thus failing to provide the intended capacity protection. Alternatively, the simplified nonlinear distribution is conservative because it ensures that $V_{L,E}$ is reached before any damage develops in any of the interior cross-frames.

Fig. 9(b) shows a simplified model to calculate the force in the first interior cross-frame. From this model, R_1 can be expressed as a ratio of the total force V

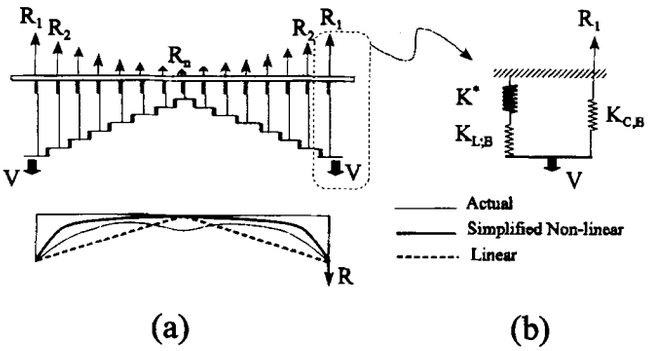

FIG. 9. (a) Force Distribution in Interior Cross-Frames; (b) Simplified Model to Calculate R_1

$$R_1 = \left(\frac{K_{C,B}}{K_{C,B} + \dfrac{K^* \cdot K_{L,B}}{K^* + K_{L,B}}}\right) \cdot V \tag{7}$$

Using a similar equation and model as (7), and deducting the force in the first interior cross-frame from the total force, the force in the second interior cross-frame becomes

$$R_2 = \left(\frac{K_{C,B}}{K_{C,B} + \dfrac{K^* \cdot K_{L,B}}{K^* + K_{L,B}}}\right) \cdot (V - R_1) \tag{8}$$

Substituting R_1 from (7) into (8) for R_2 gives

$$R_2 = V(1 - \xi)\xi \tag{9}$$

where

$$\xi = \left(\frac{K_{C,B}}{K_{C,B} + \dfrac{K^* \cdot K_{L,B}}{K^* + K_{L,B}}}\right)$$

Similarly, the force in the ith interior cross-frame is given by

$$R_i = V(1 - \xi)^{i-1}\xi \quad \text{or} \quad V = \frac{R_i}{(1 - \xi)^{i-1}\xi} \tag{10a,b}$$

If there was an infinite number of panels in the lower lateral system along the span, the preceding equations would be exact, and sum of forces in the interior cross-frames would be given by

$$\sum_{i=1}^{\infty} R_i = V\xi \sum_{i=1}^{\infty} (1 - \xi)^{i-1} = V \tag{11}$$

In reality, however, there is a finite number of interior cross-frames, and (10) actually underestimates the magnitude of the forces that would develop in the first interior cross-frame from the support for a given end shear force V. For example, if the n shown in Fig. 9(a) is equal to 4, each interior cross-frame in this deck-truss must resist a greater force to make up for the share of the load that would have been resisted by the interior cross-frames Numbers 5 to ∞. This redistribution is nonlinear and complex.

A simple procedure to obtain a conservative force distribution consists of reducing the forces in all interior cross-frames by the value needed to make the force in the central cross-frame equal to zero. Thus, if the preceding equations give a value in the central cross-frame equal to R_m, a reduced end force V', to be used for design of the retrofit system, can be calculated as follows:

$$V' = \sum_{i=1}^{m} R_i' = \sum_{i=1}^{m} (R_i - R_m) = \sum_{i=1}^{m} R_i - m \cdot R_m \tag{12}$$

Since the maximum force develops in the very first interior cross-frame, and all of these frames are typically of the same strength, it is useful to express the end force V' in terms of R_1', the force developed in the first interior cross-frame. First, substituting R_i' from (10) in (12), gives

$$V' = V\xi \left[\sum_{i=1}^{m} (1 - \xi)^{i-1} - m \cdot (1 - \xi)^{m-1}\right] \tag{13}$$

If it is known that $R_1' = R_1 - R_m = V\xi - V\xi(1 - \xi)^{m-1} = V\xi(1 - (1 - \xi)^{m-1})$, (13) expressed in terms of the first interior cross-frame force R_1' becomes

$$V' = \frac{\left(\sum_{i=1}^{m} (1 - \xi)^{i-1} - m \cdot (1 - \xi)^{m-1}\right) R_1'}{1 - (1 - \xi)^{m-1}} \tag{14}$$

Therefore, the maximum allowable end force $V_{L,E}$ is attained when the first sway-frame force reaches its strength S_{cr} (corresponding to buckling of its braced members, fracture of a nonductile connection, or other limit states), i.e.

$$V_{L,E} = \frac{\left(\sum_{i=1}^{m} (1 - \xi)^{i-1} - m \cdot (1 - \xi)^{m-1}\right) S_{Cr}}{1 - (1 - \xi)^{m-1}} \tag{15}$$

Note that if the total number of interior cross-frames, k, in a deck-truss is an even number (i.e., $m = (k + 1)/2$ is not an integer), m can be conservatively taken as $k/2$.

Given the preceding limits, the maximum total strength of the superstructure will be the sum of the limit for each retrofit component but not exceeding the substructure capacity, i.e.

$$V_{\max} \leq \min[2(V_{L,E} + V_{E,S}), 2V_{\text{Sub}}] \tag{16}$$

where V_{Sub} = largest shear that can be applied at the top of the abutment without damaging the substructure (connections, wind shoes, etc.). Eq. (16) can be easily modified for bridges having multiple simply supported spans. The value of $V_{\max}$ must also include a safety factor, as normally done in capacity design, to account for the possibility of higher than specified yield strength of the steel used in the ductile energy dissipating elements and the effects of strain hardening and strain rates. Furthermore, a minimum strength $V_{\min}$ must also be provided to resist the winds expected during the life of the structure. Therefore, the yield capacity of the overall deck-truss system should satisfy the following:

$$V_{\min} \leq R_{\text{total}} \leq V_{\max} \tag{17}$$

The chosen total strength of the retrofitted system can then be divided proportionally between the lower end and end panels according to the following equations, which ensure the same safety margin for both panels:

$$R_{L,E} = \frac{R_{\text{total}}}{V_{\max}} V_{L,E} \tag{18}$$

$$R_{E,S} = \frac{R_{\text{total}}}{V_{\max}} V_{E,S} \tag{19}$$

Dynamic Response and Determination of Period (Stiffness) Limits

A systematic approach is necessary to ensure compliance with all design constraints. The procedure proposed here uses the tripartite representation of the Newmark-Hall design elastic and inelastic response spectra, for illustration purposes.

Having found the upper and lower bounds of the total strength of the retrofitted system [by (17)], a median value can

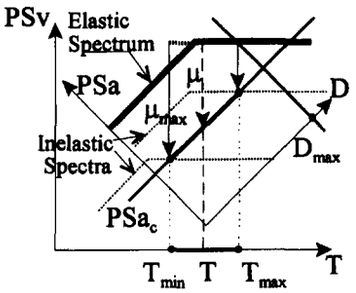

FIG. 10. Determination of Period Limits Using Capacity-Based Pseudoacceleration Line

be chosen as the desired capacity of the system. Then, a corresponding capacity-based pseudoacceleration PSa_c, can be calculated as

$$PSa_c = \frac{R_{\text{total}}}{M} \tag{20}$$

A line corresponding to that constant capacity-based pseudoacceleration can be drawn on the tripartite response spectra, as shown in Fig. 10. Every point on this line, in the short period range, corresponds to an inelastic response spectrum for a system that would develop a global ductility μ, if it had that specific yield strength; some of these spectra are drawn in dotted lines in Fig. 10. In the intermediate period range, the ductility demand of systems having a constant strength decreases as the period increases (i.e., as stiffness decreases), while their displacement response increases. Therefore, a range of admissible values can be located along the capacity-based pseudoacceleration line, based on the permissible values of global ductility and displacement of the system corresponding to a particular ductile retrofit system. Therefore, this spectra can provide guidance to select a desirable period, and the corresponding stiffness can be calculated using (5).

As shown in Fig. 10, the upper bound value for period $T_{\max}$ corresponds to the maximum drift limit, shown as $D_{\max}$ on the elastic spectra. Knowing that a Newmark-Hall inelastic pseudoacceleration spectrum is constructed by reducing the elastic spectrum values by μ (or $\sqrt{2\mu - 1}$ depending on the range of period), a lower bound to the period $T_{\min}$ can be obtained by limiting the system ductility response to the maximum permissible ductility $\mu_{\max}$ (note that, in some instances, $T_{\min}$ may not exist). As a result of these two constraints

$$T_{\min} \leq T \leq T_{\max} \tag{21}$$

Determination of Stiffness for Retrofitted Panels

To find the acceptable range of stiffness of the retrofit system, it is more convenient to express the global stiffness of the entire structural system in terms of that of the retrofitted end panel. Thus, rearranging (4) gives

$$K_{\text{Global}} = 2K_{E,S}\left(1 + \frac{K_{L,S}}{K_{E,S}}\right) \tag{22}$$

As the displacement imposed on the end panel and lower end system is the same (the top beam in the 2D model can be assumed rigid), and because the two ductile panels at each end of the span are to be designed to yield simultaneously, the stiffness ratio term $K_{L,S}/K_{E,S}$ can be replaced by the already known strength ratio $R_{L,S}/R_{E,S}$. Thus

$$K_{\text{Global}} = 2K_{E,S}\left(1 + \frac{R_{L,S}}{R_{E,S}}\right) \tag{23}$$

where, $R_{L,S}$ and $R_{E,S}$ = panel shear strength of the lower end panel and end panels, respectively. Rearranging (23) for the retrofitted end panel stiffness, gives

$$K_{E,S} = \frac{K_{\text{Global}}}{\alpha} \tag{24}$$

where

$$\alpha = 2\left(1 + \frac{R_{L,E}}{R_{E,S}}\right)$$

Thus, (21) can be expressed in terms of global stiffness, by first squaring all terms as follows:

$$T_{\min}^2 \leq T^2 \leq T_{\max}^2 \tag{25}$$

and then substituting the relevant expression for T, to obtain

$$\frac{4\pi^2 M}{T_{\max}^2} \leq K_{\text{Global}} \leq \frac{4\pi^2 M}{T_{\min}^2} \tag{26}$$

Using (24) to solve for the end panel stiffness gives

$$\frac{4\pi^2 M}{\alpha T_{\max}^2} \leq K_{E,S} \leq \frac{4\pi^2 M}{\alpha T_{\min}^2} \tag{27}$$

This can be used to select proper values of stiffness for the retrofitted end panel. To calculate the stiffness of the lower end retrofit panel $K_{L,E}$, stiffness of the lower load path system is first determined from (22)

$$K_{L,S} = \frac{K_{\text{Global}} - 2K_{E,S}}{2} \tag{28}$$

Then, because that stiffness can be considered as two springs in series, one for the retrofitted lower end panel and the other for the lower lateral interior cross-frame subsystem (i.e., the rest of the assembly), the following expression results:

$$\frac{1}{K_{L,S}} = \frac{1}{K_{L,E}} + \frac{1}{K^*} \tag{29}$$

where K^* = value of stiffness given by (3). Rearranging to solve for $K_{L,E}$ gives

$$K_{L,E} = \frac{K^* \cdot K_{L,S}}{K_{L,S} - K^*} \tag{30}$$

Using these constraints, as well as the other case-specific design requirements described earlier, the ductile retrofit systems can be designed.

NUMERICAL EXAMPLE

For the deck-truss bridge described in the second section of this paper, a generic ductile retrofit system is designed according to the procedure presented earlier. From the geometry and properties of the structural members in the existing truss, the following panel stiffnesses are calculated: $K_{C,B} = 2.349 \times 10^7$ N/m and $K_{L,B} = 4.88 \times 10^7$ N/m. Substituting these values in (2) gives a stiffness of $K^* = 4.762 \times 10^7$ N/m for the lower load path system.

A mean-plus-one-standard-deviation Newmark-Hall elastic spectra for 2% damping is then drawn using amplification factors of 3.66 and 2.92 for the acceleration and velocity parts of the spectra, respectively. Assuming that a bridge is located in a seismic region for which a peak ground acceleration of $0.4g$ is specified (by the AASHTO code for example), the resulting coordinates of this design spectra are $1.46g$ ($PSa = 3.66 \times 0.4g = 1.46g$) and 1.42 m/s ($PSv = 2.92 \times 48$ in./s $\times$ 0.4 = 56.1 in./s).

Capacity limits are then calculated. For the end cross-frames, maximum shear is $V_{E,S} \leq 1{,}545$ kN, assuming that

buckling of the verticals in the end cross-frame governs in (6). For the lower end panel, maximum shear is obtained by the following procedure. First, knowing the values of $K_{C,B}$, $K_{L,B}$, and K^*, (9) gives $\xi = 0.493$. For geometry and member sizes of the existing deck-truss, the critical panel force S_{cr} for the first interior cross-frame from the support is calculated. In this example, S_{cr} = 456 kN, corresponding to buckling of braces. Here, the total number of interior cross-frames k is 7, and $m = (k + 1)/2 = 4$. Thus (15) gives $V_{L,E} = (1.578) \times 456$ kN = 719 kN. It is then possible to calculate $V_{max} = 2(V_{L,E} + V_{E,S}) = 2(1,545 + 719) = 4,528$ kN, using (16) and assuming that shear capacity of the pier is greater than that of the superstructure. The minimum capacity for wind-load demand is $V_{min} = V_{wind} = 2,500$ kN.

Total capacity is then selected. Considering an overstrength of 50%, using (17), it is found that $R_{total} = 3,000$ kN $\leq 4,528/1.5 = 3,018$ kN and $\geq 2,500$ kN. Using (18) and (19), $R_{E,S} = 3,000/4,528 \times V_{L,E} = 1,023$ kN and $R_{L,E} = 3,000/4,528 \times V_{E,S} = 476$ kN.

Displacement and ductility limits are then verified. It is found that the maximum admissible distortion of the lower chord before it suffers damage D_1 is 0.18 m. An arbitrary limit of 2% for maximum drift of the deck relative to the support corresponds to a maximum deck drift D_2 of 0.2 m for the 10-m-high panels. Therefore, the maximum admissible displacement D_{max} is the minimum of 0.18 and 0.2 m, i.e., 0.18 m. Finally, from the maximum force modification factor (R_w = 10) permitted by Uniform Building Code, the corresponding implied maximum ductility, $\mu_{max} = 3/8 \times 10 = 3.75$, is used here.

For the total mass M of 640,000 kg and selected total capacity R_{total} of 3,000 kN, (20) gives a constant pseudoacceleration value of $PSa_c = R_{total}/M = 3,000$ kN/640,000 kg = $0.47g$. By drawing the capacity-based pseudoacceleration line on the Newmark-Hall spectrum, and considering the maximum displacement limit D_{max} of 0.18 m, a maximum period T_{max} of 0.85 s is found. From the preceding data, the maximum spectra reduction possible is $PSa/PSa_c = 1.46g/0.47g = 3.11$, which is greater than the value of $2.54 = \sqrt{2\mu - 1}$, corresponding to $\mu = \mu_{max} = 3.75$ in the short-period range of the spectra. Therefore, a minimum period T_{min} exists and is found considering the limit on maximum ductility. Here, for a maximum ductility of 3.75, T_{min} is 0.48 s.

The stiffness of the end and lower end retrofitted panel can now be determined. The value of the stiffness ratio α, calculated by (24), is $\alpha = 2 \times (1 + 476$ kN/1,023 kN) = 2.94. Eq. (27) is then used to determine an acceptable range of stiffness for the retrofitted end panel. This indicates that $1.18 \times 10^7 \leq K_{E,S} \leq 3.73 \times 10^7$ is needed. At this stage, further consideration constraints due to the type of ductile system implemented would need to be considered and could have an impact on stiffness and strength limits. A value of 3.3×10^7 N/m is selected here (which would be appropriate for an eccentrically braced frame type of ductile end panel as shown in the companion paper). Finally, the global stiffness of the deck-truss [(24)] is $K_{global} = 3.3 \times 10^7$ N/m $\cdot 2.94 = 9.7 \times 10^7$ N/m, the stiffness of the lower system assembly [(28)] is $K_{L,S} = 1.55 \times 10^7$ N/m, and stiffness of the lower end retrofitted panel [(30)] is $K_{L,E} = 2.29 \times 10^7$ N/m.

To validate this solution, the behavior of the deck-truss retrofitted with ductile devices having strength and stiffness values as calculated previously was analyzed using the nonlinear inelastic computer program DRAIN-3DX. Nonlinear dynamic time history analyses were performed, subjecting the truss to six western U.S. ground excitation records scaled to a peak ground acceleration of $0.6g$. These three-dimensional (3D) analyses showed a fundamental period of vibration for the retrofitted truss of 0.49 s [compared to the value of 0.51 s given by (5)], an average ductility demand μ of 2.68 (less than the target μ_{max} of 3.75) and a maximum end-panel displacement demand of 0.054 m (less than the maximum permissible value D_{max} of 0.18 m). As expected, there was no yielding or buckling of truss members, other than yielding in the ductile panels. Moreover, reaction forces at the truss supports did not exceed their limits, thus preventing excessive force in the substructure. To illustrate the improvement in dynamic response, the time-history of the reaction-force at the support of the retrofitted truss is compared to that of the truss having the same retrofit panels but assuming entirely elastic behavior (corresponding to a superstructure strengthening solution, where all truss members are to remain elastic). As shown in Fig. 11, due to strain hardening of the ductile device the reaction-force for the ductile retrofitted truss may slightly exceed the yield capacity of the end and lower end panels combined calculated assuming elasto-perfectly plastic behavior (1,023 + 476 $\simeq$ 1,500 kN), but it never exceeds the capacity corresponding to the failure limit states of nonductile superstructure members, or of the substructure, whichever is less (i.e., $V_{max}/2 = 4,528/2 = 2,264$ kN).

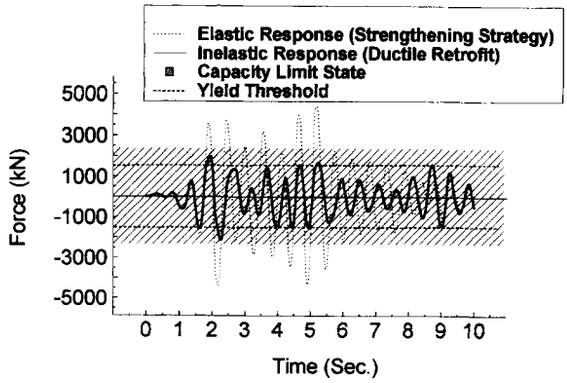

FIG. 11. Time History of Horizontal Reaction Force at Support of Deck-Truss Bridge Subjected to 0.6g El Centro Earthquake

CONCLUSIONS

A methodology is proposed to retrofit deck-truss bridges using ductile panels. It requires conversion of the two end cross-frames and the two lower lateral panels adjacent to the supports into ductile panels designed to yield and dissipate energy while preventing damage elsewhere into the superstructure or substructure, by virtue of capacity design principles. Structural interventions are minimized and limited to more accessible regions of the span.

A procedure is presented to make design possible by hand calculations. Formulas that capture the important characteristics of the transverse seismic response of deck-trusses were derived and can be used to ensure that seismic performance goals are met. Following this procedure, stiffness and strength of ductile retrofit panels needed to retrofit a 80-m-span deck-truss were determined. Computer simulations of the dynamic behavior of the retrofitted deck-truss subjected to severe ground excitation showed satisfactory performance and validated the analytical procedure for the proposed retrofit strategy.

Although the concept appears sound, further research is desirable prior to implementation. Specifically, experimental validation using 3D models is desirable, along with parametric studies to determine the range of substructure flexibility for which the retrofit solution remains effective. Finally, some of the constraints imposed here are conservative and could be relaxed if justified by future research.

APPENDIX. REFERENCES

Astaneh-Asl, A., Bolt, B., McMullin, K., Modjtahedi, D., Cho, S., and Donikian, R. (1994). "Seismic performance of steel bridges during the 1994 Northridge Earthquake." *Rep. No. UCB/CE-Steel-94/01*, Dept. of Civ. Engrg., Univ. of California, Berkeley, Calif.

Bruneau, M., Wilson, J. W., and Tremblay, R. (1996). "Performance of steel bridges during the 1995 Hyogoken-Nanbu (Kobe, Japan) earthquake." *Can. J. Civ. Engrg.*, Ottawa, Canada, 23(3), 678–713.

Capron, M. R. (1995). "Seismic evaluation and retrofit strategies for Route I-55 over the Mississippi River near Caruthersville, Missouri." *Proc., 1st Nat. Seismic Conf. on Bridges and Hwy.*, CALTRANS and FHWA, San Diego, Calif.

Housner, G., and Thiel, C. (1995). "The continuing challenge: Report on the performance of state bridges in the Northridge Earthquake." *Earthquake Spectra*, 11(4), 607–636.

Imbsen, R., and Liu, W. (1993). "Seismic evaluation of Benicia-Martinez Bridge." *Proc., 1st U.S. Seminar, Seismic Evaluation and Retrofit of Steel Bridges*, Univ. of California, Berkeley, Calif.

Imbsen, R., Schamber, R., Davis, G. (1995). "Seismic retrofit of the north approach viaduct of the Golden Gate Bridge." *Proc., 1st Nat. Seismic Conf. on Bridges and Hwy.*, San Diego, Calif.

Lui, W., Nobari, F., Schamber, A., and Imbsen, R. (1997). "Performance based seismic retrofit of Benicia-Martinez Bridge." *Proc., 2nd Nat. Seismic Conf. on Bridges and Hwy.*, CALTRANS and FHWA, Sacramento, Calif., 509–523.

Mander, J. B., Kim, D.-K., Chen, S. S., and Premus, G. J. (1996). "Response of steel bridge bearings to reversed cyclic loading." *Res. Rep. NCEER-96-0014*, Nat. Ctr. for Earthquake Engrg., State Univ. of New York at Buffalo, Buffalo, N.Y.

Matson, D. D., and Buckland, P. G. (1995). "Experience with seismic retrofit of major bridges." *Proc., 1st Nat. Seismic Conf. on Bridges and Hwy.*, CALTRANS and FHWA, San Diego, Calif.

Prakash, V., Powell, G. H., and Campbell, S. (1994). "DRAIN-3DX base program description and user guide." *Rep. No. UCB/SEMM-94/07*, Dept. of Civ. Engrg., Univ. of California, Berkeley, Calif.

Sarraf, M., and Bruneau, M. (1998). "Ductile seismic retrofit of steel deck-truss bridges. II: Design applications." *J. Struct. Engrg.*, ASCE, 124(11), 1263–1271.

Wilson, E., and Habibullah, A. (1990). "SAP90—A structural analysis program." Computers and Structures Inc., Berkeley, Calif.